

# TICRA

## In-flight Retrieval of Geometrical information on the Planck Telescope

Alternative  
Geometry retrieval  
using LFI beam data  
from all Jupiter scans

Author: Per Heighwood Nielsen

June, 2015

S-1563-12

TICRA

LÆDERSTRÆDE 34 · DK-1201 COPENHAGEN K

TELEPHONE +45 33 12 45 72

E-MAIL [ticra@ticra.com](mailto:ticra@ticra.com)

DENMARK

TELEFAX +45 33 12 08 80

<http://www.ticra.com>

VAT REGISTRATION NO. DK-1055 8697

TICRA FOND, CVR REG. NO. 1055 8697



## TABLE OF CONTENTS

1. Introduction.	1
2. LFI Retrieval with no reflector z-translations.	2
3. Comparison of LFI geometry retrievals.	6
4. HFI beam fit to LFI geometry retrieval.	8
5. Conclusion.	11
References	13



## 1. Introduction.

The present study is prepared for ESTEC under contract no. 18395/04/NL/NB, CCN no. 8.

The title of the work is

*“In-flight Retrieval of Geometrical information on the Planck Telescope”*

This Report presents an alternative retrieval of the possible telescope errors using all the measured data obtained by Jupiter LFI observations, but with no reflector z-translations at all, see Chapter 2.

This retrieval is compared in Chapter 3 with the two other LFI retrievals from Report S-1563-09, both with different fixed z-translations of the reflectors.

The HFI beam fits to these three LFI retrievals are found and compared in Chapter 4.

The Planck telescope is modelled as the in-Flight, NRFFM, configuration at operational temperature as described in TICRA Report S-1531-02 and with the new detector positions described in Report S-1563-09.

The alternative telescope geometry is retrieved in Chapter 2 using the extended version of the Physical Optics Shaping program, POS, explained in TICRA Report S-1487-04.

## 2. LFI Retrieval with no reflector z-translations.

The retrieval is performed with the extended version of the POS program using the 22 measured LFI beams as in Report S-1563-09. All observations down to 15 dB below peak are utilized. Therefore, the separate beams are only weighted proportionally to the number of observations.

Only Zernike modes up to (3,3) on both sub- and main-reflector and a rotation of the RDP coordinate system shown in Figure 2-1 are used in the retrieval.

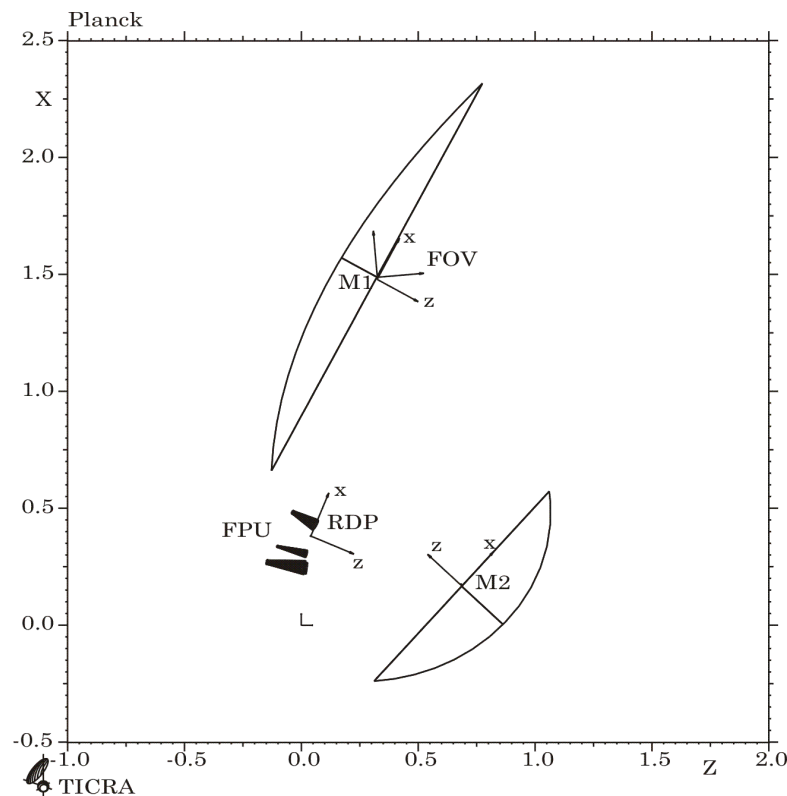


Figure 2-1 Coordinate systems in retrievals.

As in Report S-1563-09 the RFFM telescope geometry is corrected with the new locations of the LFI detectors in the FPU system (NRFFM).

The 1st retrieval is performed with the FPU fixed but in the corrected NRFFM feed positions. Only a rotation of the FPU around its z-axis is performed.

All detectors, except the two very direction-diverging detectors LFI20S and LFI21S are used in the 1<sup>st</sup> retrieval of the telescope geometry.

After this 1st retrieval the detector positions in x- and y-direction are retrieved for all beams and a better fit of the beam shapes is now possible by replacing the detectors to the retrieved positions and resuming the retrieval of the surface distortions.

The surface distortions found in this new retrieval are shown in Table 2-1 and Table 2-2.

Zernike mode		Amplitude	Rotation
m	n	[mm]	[degrees]
0	0	0.0	0
0	2	-0.13	0
1	1	1.12	51
2	2	0.08	62
1	3	0.05	-6
3	3	0.02	-25

Table 2-1 Retrieved Zernike modes on main reflector.

Zernike mode		Amplitude	Rotation
m	n	[mm]	[degrees]
0	0	0.0	0
0	2	0.06	0
1	1	1.79	-25
2	2	0.06	-18
1	3	0.31	-3
3	3	0.05	32

Table 2-2 Retrieved Zernike modes on subreflector.

The retrieved Zernike distorted surfaces without the Zernike modes (0,0) and (1,1) are shown in Figure 2-2 and Figure 2-3 for main and sub-reflector, respectively.

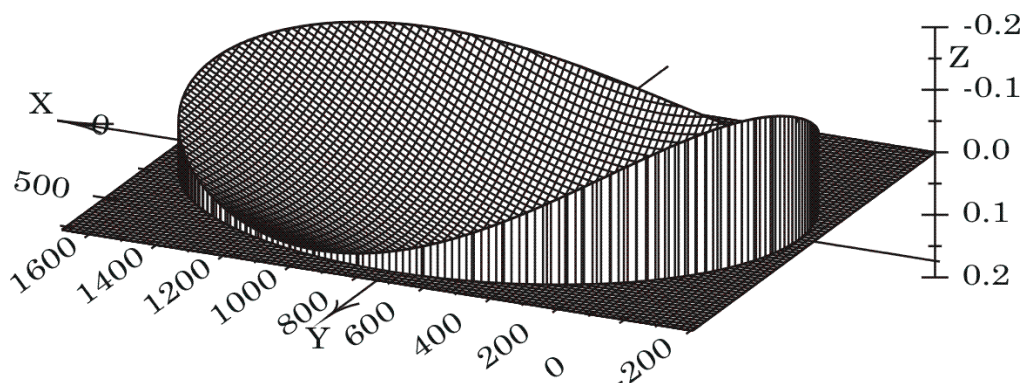


Figure 2-2 Retrieved main reflector surface deformations.

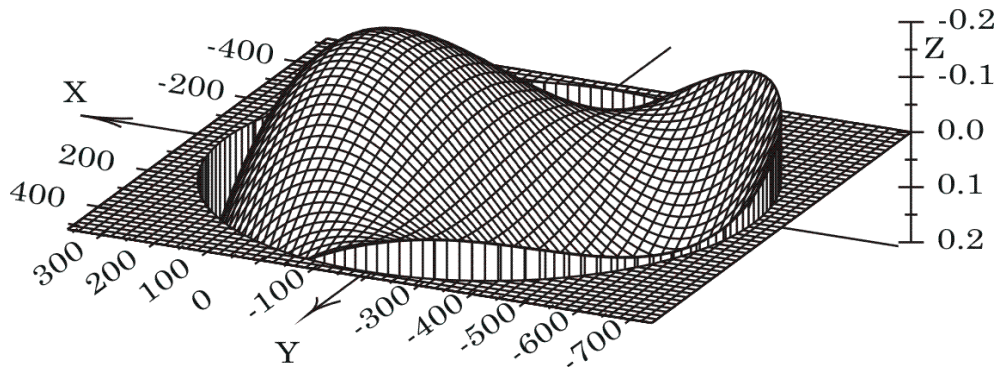


Figure 2-3 Retrieved subreflector surface deformations.

The maximum rim distortions are  $\pm 0.21$  mm and  $\pm 0.18$  mm for sub- and main-reflector, respectively. The large curvature on the main reflector is due to a combination of Zernike modes (0,2) and (2,2). On the subreflector it is the Zernike mode (1,3).

The maximum feed displacements can be reduced by retrieval of the FPU coordinate system with constraints on the possible feed displacements. Again the detectors LFI20S and LFI21S are too dislocated to be used in this retrieval of the FPU.

The resultant position of the FPU relative to the RDP coordinate system is retrieved to:

- 1) translation in x-direction of  $\pm 0.06$  mm
- 2) translation in y-direction of  $\pm 0.01$  mm
- 3) translation in z-direction of  $+0.05$  mm
- 4) rotation around the z-axis of  $\pm 4.1$  arcmin

With this FPU position all the remaining feed displacements are retrieved in Table 2-3



Feed displacements	Deviation from retrieved RDP	
	$\Delta x$ [mm]	$\Delta y$ [mm]
LFI18	0.05	0.12
LFI19	0.10	-0.12
LFI20	0.18	0.35
LFI21	-0.42	-0.35
LFI22	0.07	0.08
LFI23	0.13	-0.01
LFI24	-0.08	-0.14
LFI25	-0.10	-0.07
LFI26	0.02	0.06
LFI27	-0.06	0.14
LFI28	0.08	0.10

Table 2-3 Final retrieved feed displacements.

Due to the averaging, the translation limits are now reduced to  $\pm 0.13$  mm in x-direction and  $\pm 0.14$  mm in y-direction for all the detectors except for LFI20 and LFI21.

The resultant remaining beam variances down to the 15 dB level are listed in Table 2-4. The total variance for all beams is 0.089 dB.

Detector	Variance $\delta$ [dB]	
	S-pol	M-pol
LFI18	0.08	0.07
LFI19	0.05	0.07
LFI20	0.04	0.04
LFI21	0.06	0.05
LFI22	0.07	0.05
LFI23	0.06	0.08
LFI24	0.08	0.06
LFI25	0.11	0.12
LFI26	0.10	0.17
LFI27	0.12	0.10
LFI28	0.13	0.11
Total	0.089 dB	

Table 2-4 Remaining variances from retrieval of reflector surface distortions and feed displacement.

### 3. Comparison of LFI geometry retrievals.

The retrieval with no reflector translation presented above is compared with the other LFI retrievals in Report S-1563-09. Here the z-translations are here -0.3 mm to -0.9 mm of the main reflector and -0.6 mm to -1.8 mm of the sub reflector. The retrieved Zernike modes are summarized in Table 3-1.

Zernike Modes	Amplitude [mm]			Phase [deg]		
Main	M.0 -S.0	M.3 - S.6	M.9 - S.1.8	M.0 -S.0	M.3 - S.6	M.9 - S.1.8
0 0	0.00	-0.30	-0.90	0	0	0
0 2	-0.13	-0.15	-0.20	0	0	0
1 1	1.09	1.11	1.02	55	54	62
1 3	0.06	0.06	0.09	1	-5	-4
2 2	0.05	0.08	0.07	45	59	51
3 3	0.02	0.02	0.02	-52	-27	-30
Sub						
0 0	0.00	-0.60	-1.80	0	0	0
0 2	0.03	-0.02	-0.18	0	0	0
1 1	1.67	1.76	1.69	-28	-26	-26
1 3	0.32	0.28	0.22	-6	-4	-5
2 2	0.05	0.08	0.11	-54	-13	-8
3 3	0.06	0.05	0.05	54	32	31

Table 3-1 LFI retrieved Zernike modes.

The differences are noticed to be very small. Only the Zernike mode (0,2) marked in red is changed significantly for the largest translation (M.9-S1.8).

The retrieved corrections of the RDP coordinate system are given in Table 3-2 showing no significant changes.

Retrieved LFI RDP deviations			
	M.0 -S.0	M.3 - S.6	M.9 - S1.8
x-translation	-0.06 mm	-0.06 mm	-0.04 mm
y-translation	-0.01 mm	-0.02 mm	-0.01 mm
z-translation	0.05 mm	0.06 mm	0.08 mm
rotation	-4.1 arcmin	-4.4 arcmin	-4.2 arcmin

Table 3-2 Retrieved LFI RDP coordinate system deviations.

The remaining detector position displacements from the new positions (NRFFM) are presented in Table 3-3.

LFI	Deviation in retrieved RDF coordinate system					
	$\Delta x$ [mm]			$\Delta y$ [mm]		
Detector	M.0 -S.0	M.3 - S.6	M.9 - S.1.8	M.0 -S.0	M.3 - S.6	M.9 - S.1.8
LFI18	0.05	0.06	0.02	0.12	0.13	0.11
LFI19	0.10	0.11	0.07	-0.12	-0.11	-0.12
LFI20	0.18	0.19	0.15	0.35	0.36	0.35
LFI21	-0.42	-0.41	-0.45	-0.35	-0.34	-0.35
LFI22	0.07	0.07	0.03	0.08	0.09	0.08
LFI23	0.13	0.13	0.10	-0.01	0.00	0.00
LFI24	-0.08	-0.06	-0.08	-0.14	-0.13	-0.14
LFI25	-0.10	-0.10	-0.09	-0.07	-0.06	-0.06
LFI26	0.02	0.04	0.03	0.06	0.08	0.04
LFI27	-0.06	-0.05	-0.06	0.14	0.14	0.14
LFI28	0.08	0.10	0.08	0.10	0.11	0.10
Average	0.00	0.01	-0.02	0.02	0.02	0.01
Peak to Peak	0.23	0.23	0.19	0.28	0.27	0.28

Table 3-3 Retrieved LFI detector position displacements.

The displacements for the very diverging detectors LFI20 and LFI21 are marked in orange and are omitted in the peak to peak calculation. Again the differences are very small. This is also the case for the remaining beam variations in Table 3-4.

LFI	Variance $\delta$ [dB]					
polarisation	S-pol			M-pol		
Detector	M.0 -S.0	M.3 - S.6	M.9 - S.1.8	M.0 -S.0	M.3 - S.6	M.9 - S.1.8
LFI18	0.08	0.08	0.07	0.07	0.07	0.06
LFI19	0.05	0.05	0.04	0.07	0.07	0.07
LFI20	0.04	0.03	0.03	0.04	0.04	0.04
LFI21	0.06	0.06	0.06	0.05	0.04	0.05
LFI22	0.07	0.07	0.06	0.05	0.05	0.05
LFI23	0.06	0.06	0.05	0.08	0.07	0.07
LFI24	0.08	0.07	0.07	0.06	0.06	0.07
LFI25	0.11	0.10	0.10	0.12	0.11	0.11
LFI26	0.10	0.10	0.09	0.17	0.16	0.16
LFI27	0.12	0.12	0.12	0.10	0.10	0.10
LFI28	0.13	0.13	0.13	0.11	0.11	0.11
Total	0.089	0.087	0.084	0.089	0.087	0.084

Table 3-4 Remaining residuals in the LFI retrievals.

#### 4. HFI beam fit to LFI geometry retrieval.

When fitting the selected HFI beams in Report S-1563-11 to the 3 different retrieved LFI configurations and allowing a rotation of the common RDP coordinate system for the HFI detectors the resulting remaining deviations of the HFI beam directions presented in Table 4-1 are found.

RFFM & LFI	Deviation of output directions [arcsec]					
Beam directions	Cx-scan			Co-scan		
Detector	M.0 -S.0	M.3 - S.6	M.9 - S.1.8	M.0 -S.0	M.3 - S.6	M.9 - S.1.8
HFI-100-2a	24	23	20	-10	-9	-7
HFI-100-2b	24	23	20	-8	-7	-4
HFI-100-4a	14	13	12	-11	-10	-9
HFI-100-4b	13	13	11	-10	-9	-7
HFI-143-1a	36	34	30	-14	-14	-15
HFI-143-1b	38	36	32	-12	-13	-14
HFI-143-4a	29	28	26	-14	-14	-16
HFI-143-4b	27	26	25	-12	-12	-14
HFI-143-5	35	34	31	-7	-8	-10
HFI-143-6	30	29	26	-23	-24	-26
HFI-217-1	38	36	32	-14	-13	-11
HFI-217-4	22	20	17	4	5	7
HFI-353-1	54	49	38	-13	-11	-7
HFI-353-2	58	52	40	-11	-9	-6
HFI-353-6a	47	41	31	1	0	-2
HFI-353-6b	47	42	32	-3	-4	-6
Average	34	31	26	-10	-10	-9

Table 4-1 HFI beam deviations in arc seconds.

The beam direction deviations are all very similar. Only in the Cx-scan direction the deviations are slightly decreasing for increasing z-translations. The large average output deviations of around 30 arcsec in Cx- and -10 arcsec in Co-direction are generating the retrieved x and y depositions in Table 4-2 of the HFI RDP coordinate system relative to the common FPU coordinate system.

Retrieved HFI RDP deviations			
	M.0 -S.0	M.3 - S.6	M.9 - S1.8
x-translation	0.29 mm	0.28 mm	0.22 mm
y-translation	-0.08 mm	-0.08 mm	-0.07 mm
z-translation	0.40 mm	0.30 mm	0.07 mm
rotation	-2.2 arcmin	-2.4 arcmin	-3.6 arcmin

Table 4-2 Retrieved HFI RDP coordinate system deviations.

Especially, the HFI z-translation for the LFI retrievals is dissimilar giving 0.1 mm lesser displacement for the M.3\_S.6 case and nearly no translation for the M.9\_S1.8 case. Instead the RPD rotation is increased to -3.6 arcmin (marked orange) for the M.9\_S1.8 case. This large rotation is in fact nearly the same size as the RDP rotation for the LFI retrieval (-4.2 arcmin). Table 4-3 shows the deviations of the RDP coordinate system for the HFI detectors in relation to the RDP coordinate system from the LFI retrievals.

Retrieved HFI RDP deviations relative to LFI			
	M.0 -S.0	M.3 - S.6	M.9 - S1.8
x-translation	0.35 mm	0.35 mm	0.26 mm
y-translation	-0.07 mm	-0.06 mm	-0.06 mm
z-translation	0.36 mm	0.24 mm	0.06 mm
rotation	+2.1 arcmin	+2.0 arcmin	+0.6 arcmin

Table 4-3 Relative deviations of the HFI RDP coordinate system.

The remaining HFI detector displacements in the repositioned HFI RDP coordinate systems are retrieved in Table 4-4 with the deviations larger than 0.1 mm marked in orange..

HFI detector deviation in RDF using the 3 LFI retrieval geometries						
	$\Delta x$ [mm]			$\Delta y$ [mm]		
Detector	M.0 -S.0	M.3 - S.6	M.9 - S1.8	M.0 -S.0	M.3 - S.6	M.9 - S1.8
HFI-100-2	-0.04	-0.05	-0.03	0.04	0.04	0.01
HFI-100-4	-0.11	-0.12	-0.11	0.00	0.00	-0.01
HFI-143-1	-0.06	-0.05	0.03	0.00	0.00	-0.02
HFI-143-4	-0.07	-0.07	-0.03	-0.08	-0.06	-0.04
HFI-143-5	-0.08	-0.07	0.02	0.04	0.03	0.02
HFI-143-6	-0.12	-0.11	-0.03	-0.12	-0.12	-0.12
HFI-143-7	-0.08	-0.07	0.00	-0.14	-0.13	-0.12
HFI-217-1	0.05	0.04	0.07	0.00	0.00	-0.02
HFI-217-4	-0.07	-0.09	-0.08	0.11	0.12	0.11
HFI-353-1	0.12	0.10	0.11	0.03	0.04	0.03
HFI-353-2	0.15	0.13	0.12	0.03	0.04	0.03
HFI-353-6	0.10	0.07	0.03	0.05	0.05	0.04
Average	-0.02	-0.02	0.01	0.00	0.00	-0.01
Peak to peak	0.27	0.24	0.24	0.23	0.24	0.23

Table 4-4 Retrieved feed displacements in the HFI retrieved telescope geometry.

The remaining residuals are given in Table 4-5

HFI	Variance $\delta$ [dB]		
Detector	M.0 -S.0	M.3 - S.6	M.9 - S1.8
HFI-100-2a	0.30	0.30	0.30
HFI-100-2b	0.30	0.30	0.30
HFI-100-4a	0.25	0.25	0.25
HFI-100-4b	0.24	0.24	0.24
HFI-143-1a	0.47	0.45	0.42
HFI-143-1b	0.48	0.46	0.44
HFI-143-4a	0.76	0.73	0.68
HFI-143-4b	0.78	0.76	0.70
HFI-143-5	0.59	0.57	0.54
HFI-143-6	0.75	0.73	0.69
HFI-143-7	0.70	0.68	0.64
HFI-217-1	0.52	0.52	0.51
HFI-217-4	0.65	0.63	0.61
HFI-353-1	0.69	0.67	0.65
HFI-353-2	0.93	0.90	0.83
HFI-353-6a	0.94	0.88	0.77
HFI-353-6b	0.96	0.91	0.81
Average	0.65	0.63	0.58

Table 4-5 Beam residuals down to 20 dB power level.

Also, as shown for the LFI beams, the residuals are smallest for the largest reflector z-translations in the case of the HFI beams.

## 5. Conclusion.

The three retrieved disalignments of the telescope geometry are shown to be very similar. Only the Zernike mode (0,2) is much larger (-0.18 mm) for the LFI retrieval with the largest reflector z-translation (M.9-S1.8), see Table 5-1. This and the very large reflector z-translations are ruling out this retrieval. The two other retrievals are very similar, yet the one with no reflector translation has slightly larger residuals and a larger z-translation of the HFI detectors.

The differences from the former retrievals are mainly due to the following changes:

1. The large correction of the HFI beam directions in the In-scan direction.
2. The change of the LFI detector positions of 1 mm towards the subreflector.
3. The stacked LFI and HFI beam data.
4. The new selection of the HFI beams.

Reflector z-translations	M.0 -S.0	M.3 - S.6	M.9 - S1.8
PR Zernike Modes	Amplitude [mm]		
0 0	0.00	-0.30	-0.90
0 2	-0.13	-0.15	-0.20
1 1	1.09	1.11	1.02
1 3	0.06	0.06	0.09
2 2	0.05	0.08	0.07
3 3	0.02	0.02	0.02
SR Zernike Modes			
0 0	0.00	-0.60	-1.80
0 2	0.03	-0.02	-0.18
1 1	1.67	1.76	1.69
1 3	0.32	0.28	0.22
2 2	0.05	0.08	0.11
3 3	0.06	0.05	0.05
Retrieved LFI RDP deviations			
x-translation	-0.06 mm	-0.06 mm	-0.04 mm
y-translation	-0.01 mm	-0.02 mm	-0.01 mm
z-translation	0.05 mm	0.06 mm	0.08 mm
rotation	-4.1 arcmin	-4.4 arcmin	-4.2 arcmin
Retrieved HFI RDP deviations			
x-translation	0.29 mm	0.28 mm	0.22 mm
y-translation	-0.08 mm	-0.08 mm	-0.07 mm
z-translation	0.40 mm	0.30 mm	0.07 mm
rotation	-2.2 arcmin	-2.4 arcmin	-3.6 arcmin
Deviation in retrieved LFI RDF coordinate system			
Peak to Peak $\Delta x$	0.23 mm	0.23 mm	0.19 mm
Peak to Peak $\Delta y$	0.28 mm	0.27 mm	0.28 mm
Deviation in retrieved HFI RDF coordinate system			
Peak to Peak $\Delta x$	0.27 mm	0.24 mm	0.24 mm
Peak to Peak $\Delta y$	0.23 mm	0.24 mm	0.23 mm
Retrieved variance $\delta$			
All LFI beams	0.089 dB	0.087 dB	0.084 dB
Selected HFI beams	0.65 dB	0.63 dB	0.58 dB

Table 5-1 Results of the three LFI retrievals.



## References

ESA (2000)

“Planck Telescope Design Specification”  
SCI-PT-RS-07024, dated 31/08/00.

P. Nielsen, 2009

“In-flight Retrieval of Geometrical information on the  
Planck Telescope – Retrieval of geometrical information  
and evaluation of results”, S-1487-04, dated February  
2009.

P. Nielsen, 2010

“In-flight Retrieval of Geometrical information on the  
Planck Telescope – Evaluation of weight influence”,  
S-1531-02, dated Marts 2010.

Fabrizio Villa, 2014

“LFI phase centre horn positions”, e-mail correspondence,  
March 25, 2014.

P. Nielsen, 2014

“In-flight Retrieval of Geometrical information on the  
Planck Telescope – Geometry retrieval using LFI beam  
data from all Jupiter scans”, S-1563-09, dated September  
2014.

P. Nielsen, 2015

“In-flight Retrieval of Geometrical information on the  
Planck Telescope – Geometry retrieval using new HFI  
beam data from all Saturn scans, S-1563-11, dated June  
2015.